Jpn. J. Cancer Res. **91**, 1303–1313, December 2000

A Computational Model for Quantitative Analysis of Cell Cycle Arrest and Its Contribution to Overall Growth Inhibition by Anticancer Agents

Hyo-Jeong Kuh,[1] Shin-ichi Nakagawa,[2] Jitsuo Usuda,[3] Katsunori Yamaoka,[4] Nagahiro Saijo[3] and Kazuto Nishio[3, 5]

[1]Catholic Research Institutes of Medical Science, Catholic University of Korea, 505 Banpo-dong, Seocho-ku, Seoul 137-701, Korea, [2]Cancer Information and Epidemiology Division, [3]Pharmacology Division, National Cancer Center Research Institute, 5-1-1 Tsukiji, Chuo-ku, Tokyo 104-0045 and [4]Department of Electrical and Electronic Engineering, Faculty of Engineering, Tokyo Institute of Technology, 2-12-1 Ookayama, Meguro-ku, Tokyo 152-8552

Most anticancer agents induce cell cycle arrest (cytostatic effect) and cell death (cytotoxic effect), resulting in the inhibition of population growth of cancer cells. When asynchronous cells are to be examined, the currently used flow cytometric method can not provide checkpoint-specific and quantitative information on the drug-induced cell cycle arrest. Hence, despite its significance, no good method to analyze in detail the mechanism of cell cycle arrest and its contribution to overall growth inhibition induced by an anticancer agent has yet been established. We describe in this study the development of a discrete time (Markov model)-based computational model for cell cycle progression/arrest with transition probability (TP_i) as a model parameter. TP_i was calculated using model equations that include easily measurable parameters such as the fraction of cells in each cell cycle phase and population doubling time. The TP_i was then used to analyze checkpoint-specific and quantitative changes in cell cycle progression. We also used TP_i in a Monte-Carlo simulation to predict growth inhibition caused by cell cycle arrest only. Human SCLC cells (SBC-3) exposed to UCN-01 were used to validate the model. The model-predicted growth curves agreed with the observed data for SBC-3 cells not treated or treated at a cytostatic concentration (0.2 μM) of UCN-01, indicating validity of the present model. The changes in TP_i indicated that UCN-01 reduced the G_1-to-S transition rate and increased the S-to-G_2/M and G_2/M-to-G_1 transition rates of SBC-3 cells in a concentration- and time-dependent manner. When the model-predicted growth curves were compared with the observed data for cells treated at a cytotoxic concentration (2 μM), they suggested that 22% out of 65% and 32% out of 73% of the growth inhibition could be attributed to the cell cycle arrest effect after 48 h and 72 h exposure, respectively. In conclusion, we report here the establishment of a novel method of analysis that can provide checkpoint-specific and quantitative information about cell cycle arrest induced by an anticancer agent and that can be used to assess the contribution of cell cycle arrest effect to the overall growth inhibition.

Key words: Transition probability — Computational model — Cell cycle arrest — UCN-01 — Cytostatic effect

Most anticancer agents are designed to induce cell cycle dysregulation in cancer cells, in order to cause cell cycle perturbation or arrest (cytostatic effect) and eventually cell death (cytotoxic effect). Growth inhibition, i.e., reduction in growth rate of a cell population following drug treatment in comparison to untreated cells, is the result of both effects. Neither experimental nor mathematical methods have been established yet that would separate and quantify the degree of growth inhibition caused by each of these two effects separately. The reason is two-fold. First, there was no experimental method available to quantify cell death (apoptosis), because there was no surrogate marker known to be proportional to the number of cells removed from the population in a given time period. Second, no mathematical method was available to calculate the level of growth rate reduction directly caused by cell cycle arrest. A flow-cytometry DNA histogram of asynchronously growing cells only provides limited information such as changes in the cell cycle distribution of a cell population. Using these data alone, detailed information, including the identification of the affected cell cycle checkpoints and the degree of the changes, could not be determined. Without the checkpoint-specific and quantitative data, no mathematical model could be applied, and the reduction in growth rate directly caused by cell cycle arrest could not be estimated.

The goal of the present study was to establish a mathematical method to assess the respective contributions of cell cycle arrest and cell kill effect to the overall growth inhibition induced by an anticancer agent. In order to achieve this goal, a checkpoint-specific and quantitative

[5] To whom requests for reprints should be addressed.
E-mail: knishio@gan2.res.ncc.go.jp

parameter was required. We developed a cell cycle-based computational model that uses a quantitative model parameter, the transition probability (TP_i) for cell cycle progression at each cell cycle checkpoint. The TP_i was calculated using model equations and cell cycle distribution data obtained from flow cytometry and population doubling time. Using TP_i in a Monte-Carlo simulation, the growth of a cell population grown under cell cycle arresting conditions was predicted. Therefore, the difference between the observed growth of an untreated cell population and the model-predicted population growth for treated cells represents the growth inhibition resulting from the cytostatic effect of cell cycle arrest. Note that cell number reduction by cell death is not included in the simulation. Thus, the model simulation would overestimate the growth of a population when there is cell death in the population. Hence, the difference between the model-predicted and the observed growth rate of a treated cell population represents the growth inhibition resulting solely from the cytotoxic effect of cell kill. The relative contribution of the cytostatic and the cytotoxic effects of anticancer agents to the overall growth inhibition can thus be determined.

To demonstrate the validity and applicability of the present model, a new anticancer agent, UCN-01 (7-hydroxystaurosporine),[1–3] was used as a model drug. UCN-01 is an indolocarbazole derivative currently under phase I/II studies in the US and Japan. UCN-01 was selected as a model drug for the present study, because it is understood that UCN-01 targets unique aspects of cell cycle regulation in comparison to other anticancer agents.[4] UCN-01 has been shown to inhibit progression through G_1[5] and to abrogate the G_2 checkpoint of cells exposed to DNA-damaging agents.[6, 7] Recently, UCN-01 has been studied extensively to assess its cell cycle modulatory effect in combination with other chemotherapeutic agents.[6, 8–10]

As demonstrated towards the end of this paper, our method can easily generate the growth curve of a cell population during or after various drug exposures, as long as experimental data such as cell cycle distribution after drug exposure and population doubling time of untreated cells are provided. By using the discrete time Markov model and numerical simulation, the present model eliminates complicated mathematical work and does not require comprehensive statistical understanding. Therefore, the present model is very useful not only to provide the checkpoint-specific and quantitative information about cell cycle arrest, but also to assess the contribution of cell cycle arrest effect to the overall growth inhibition induced by an anticancer agent *in vitro*.

MATERIALS AND METHODS

Drugs and reagents UCN-01 and staurosporine were kindly provided by Kyowa Hakko Kogyo Ltd. (Tokyo). UCN-01 was dissolved in dimethylsulfoxide and diluted with culture medium. Other drugs and reagents, unless otherwise noted, were purchased from Sigma Chemical Co. (St. Louis, MO).

Cell culture A human small cell lung cancer (SCLC) cell line SBC-3 was obtained from Dr. Kimura (Okayama University, School of Medicine, Okayama). A human leukemia cell line HL-60 was obtained from ATCC. Cells were maintained in RPMI1640 supplemented with 10% heat-inactivated fetal bovine serum, 100 mg/ml streptomycin, and 100 units/ml penicillin in a humidified air containing 5% (v/v) CO_2 at 37°C.

MTT growth inhibition assay The 3-(4,5-dimethyl-2-thiazolyl)-2,5-diphenyl-2H-tetrazolium bromide (MTT) assay of the growth inhibitory effect of UCN-01 was carried out as described previously.[11] Cells were seeded at a density of 2000–4000 cells/well 24 h prior to drug exposure. The cells were then treated with various concentrations of UCN-01 for up to 72 h. The absorbance of the reaction mixture was measured at 562 and 630 nm and the IC_{50} was determined as the drug concentration required to reduce the absorbance to 50% as compared to the control in each test.

Determination of population growth rate and cell cycle distribution Cells were plated at 1×10^6 to 5×10^6 cells per plate in 100 mm or 150 mm petri dishes at least 24 h prior to drug exposure. Following drug exposure, the cells were harvested at predetermined times and suspended as single cells in phosphate-buffered saline (PBS). An aliquot was used to determine total cell number using a Coulter Counter (Coulter Electronics Ltd., Luton, UK) and viable cell number by trypan blue exclusion. The rest of the cells were washed with ice-cold PBS, fixed in 5 ml of 50% methanol/PBS and stored at −20°C for up to 7 days until further analysis. For cell cycle analysis, 5×10^6 fixed cells were washed once in 5 ml of 30% methanol/PBS and twice in 5 ml of PBS. They were then re-suspended in 1ml of boiled RNase A (1 mg/ml) solution. After a 30 min incubation at 37°C, the cells were washed in PBS and stained with 2 ml of ethidium bromide (50 μg/ml) for 20–30 min on ice and protected from light. The cell cycle distribution was analyzed by flow cytometry (FACScan, Becton Dickinson Immunocytometry Systems, San Jose, CA) and cell cycle analysis software (Modfit, Verity, Topsham, ME).

Model development

Smith and Martin's cell cycle model: To describe population heterogeneity with respect to cell cycle times, a plausible hypothesis is the transition probability model of Smith and Martin.[12] This model assumes that cell cycle time variability resides predominately in the G_1 phase. The cell cycle progression is divided into a probabilistic A-state, which is contained within the G_1 phase, and a deterministic B-phase, which encompasses the remainder of the

G_1 phase and the S, G_2 and M phases. The concept of transition probability, P (h^{-1}) is defined as

$$P=\{(\alpha(t)-\alpha(t+\Delta t))/\alpha(t)\}/\Delta t \qquad \text{(Eq. 1)}$$

where $\alpha(t)$=% cells remaining undivided at time t and Δt=unit time.

This model has been verified in subsequent experiments [13–15] and the concept of transition probability has been successfully employed in many cell cycle studies, e.g., measuring G_1 exit rate and estimating DNA synthesis rate, indicating the feasibility of using the Smith and Martin's model in cell cycle analysis.

Transition probability model for cell cycle arrest: We expanded Smith and Martin's transition probability (P) and set up a transition probability for each transition phase (TP_i, Fig. 1A). In the present model, TP_i (h^{-1}) is defined as

$$TP_i(t)=\{(\alpha_i(t)-\alpha_i(t+\Delta t))/\alpha_i(t)\}/\Delta t \qquad \text{(Eq. 2)}$$

where $\alpha_i(t)$=[$N_i(t)$−(# cells already exiting from i phase at time t)]/$N_i(t)$ and $N_i(t)$=number of cells in i phase at time t (Fig. 1B). The model assumptions are: (1) exponential growth of a cell population with a growth rate constant (k), i.e., $N(t)=N(0)\cdot e^{(k\cdot t)}$, where k=ln2/(population doubling time) (Eq. 3); (2) all cells are in cycle, i.e., no cells killed and no arrest in G_0 phase; (3) distribution of cell numbers in a cell cycle follows the age structure of a simple exponential population.[16]

Model equations: According to the model assumptions and parameter definitions, mass balance equations for cell numbers in each cell cycle phase were written as follows.

$$N_{G1}(t+\Delta t)=N_{G1}(t)\cdot(1-TP_{G1}\cdot\Delta t)+2\cdot TP_{G2/M}\cdot\Delta t\cdot N_{G2/M}(t) \qquad \text{(Eq. 4.1)}$$
$$N_S(t+\Delta t)=N_S(t)\cdot(1-TP_S\cdot\Delta t)+TP_{G1}\cdot\Delta t\cdot N_{G1}(t) \qquad \text{(Eq. 4.2)}$$
$$N_{G2/M}(t+\Delta t)=N_{G2/M}(t)\cdot(1-TP_{G2/M}\cdot\Delta t)+TP_S\cdot\Delta t\cdot N_S(t) \qquad \text{(Eq. 4.3)}$$

where $N_i(t)=N_{total}(t)\cdot F_i(t)$. $N_{G1}(t)$, $N_S(t)$ and $N_{G2/M}(t)$ denote the number of cells in G_1, S and G_2/M phase at time t, respectively. TP_{G1}, TP_S, and $TP_{G2/M}$ denote the transition probability from G_1 to S, S to G_2/M, G_2/M to G_1, respectively. Eqs. (4.1) to (4.3) were solved for TP_i,

$$TP_{G1}(t)=\{(e^{(\Delta t\cdot k(t))}-1)\cdot(2-F_{G1})\}/(F_{G1}\cdot\Delta t) \qquad \text{(Eq. 5.1)}$$
$$TP_S(t)=\{(e^{(\Delta t\cdot k(t))}-1)\cdot(1+F_{G2/M})\}/(F_S\cdot\Delta t) \qquad \text{(Eq. 5.2)}$$
$$TP_{G2/M}(t)=(e^{(\Delta t\cdot k(t))}-1)/(F_{G2/M}\cdot\Delta t) \qquad \text{(Eq. 5.3)}$$

Based on a discrete-time Markov model, $TP_i(t)$ is defined for a discrete time interval of 1 h (Δt=1 h), and $TP_i(t)$ can be calculated when $F_i(t)$ and $k(t)$ are provided. $F_i(t)$ is obtained from flow cytometry and $k(t)$ either from the actual growth rate constant for control cell population or from the relative growth rate estimated by numerical simulation for treated cell populations as described below. (see 'Estimation of growth rate constant (k)').

Estimation of growth rate constant (k): In order to estimate the growth rate constant (k) of treated cells, similar

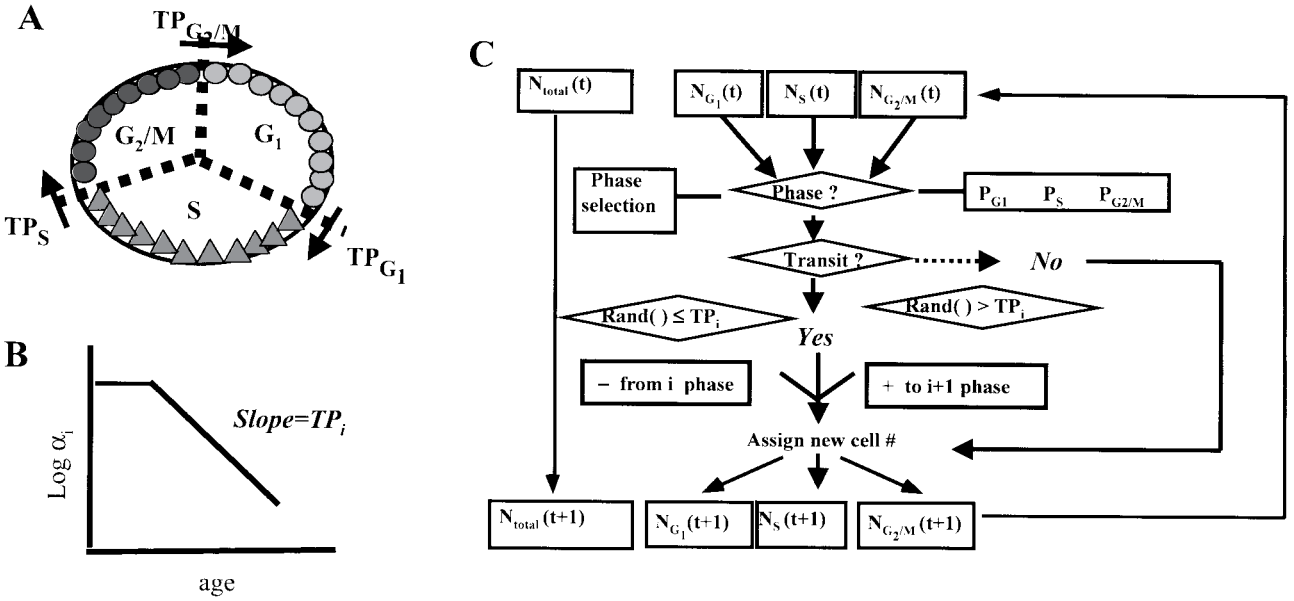

Fig. 1. Cytostatic TP_i model. (A) Schematic view of the transition probability (TP_i) concept in cell cycle progression. (B) Illustration of TP_i. The α_i is the percent remaining unexited from the phase i at time t (see 'Model development'). The slope represents TP_i.[16] (C) Algorithm of the numerical simulation for cell population growth using TP_i. A random number generator was used for phase selection and for determination of phase transition.

mass balance equations for F_i can be written when dividing Eqs. (4.1) to (4.3) by $N_{total}(t)$ as follows.

$$F_{G1}(t+\Delta t)=F_{G1}(t)\cdot(1-TI_{G1}\cdot\Delta t)+TI_{G2/M}\cdot\Delta t\cdot F_{G2/M}(t) \quad \text{(Eq. 6.1)}$$
$$F_{S}(t+\Delta t)=F_{S}(t)\cdot(1-TI_{S}\cdot\Delta t)+TI_{G1}\cdot\Delta t\cdot F_{G1}(t) \quad \text{(Eq. 6.2)}$$
$$F_{G2/M}(t+\Delta t)=F_{G2/M}(t)\cdot(1-TI_{G2/M}\cdot\Delta t)+TI_{S}\cdot\Delta t\cdot F_{S}(t) \quad \text{(Eq. 6.3)}$$

As for TP_i, $F_i(t)$ is a constant within the time unit of 1 h. TI_{G1}, TI_S and $TI_{G2/M}$ denote the relative transition probabilities (transition index) of transition from G_1 to S, S to G_2/M and G_2/M to G_1 phase, respectively, i.e., the sum of these TI_i values is equal to 1 at any given time interval. The sum of $F_{G1}(t)$, $F_S(t)$ and $F_{G2/M}(t)$ also equals 1 by definition, hence, the Eqs. (6.1) to (6.3) can be solved for TI_i as shown below.

$$TI_{G1}=F_S\cdot F_{G2/M}/(F_{G1}\cdot F_S+F_S\cdot F_{G2/M}+F_{G2/M}\cdot F_{G1}) \quad \text{(Eq. 7.1)}$$
$$TI_S=F_{G1}\cdot F_{G2/M}/(F_{G1}\cdot F_S+F_S\cdot F_{G2/M}+F_{G2/M}\cdot F_{G1}) \quad \text{(Eq. 7.2)}$$
$$TI_{G2/M}=F_{G1}\cdot F_S/(F_{G1}\cdot F_S+F_S\cdot F_{G2/M}+F_{G2/M}\cdot F_{G1}) \quad \text{(Eq. 7.3)}$$

Using these equations and Steel's age structure theory (assumption #3), the relative cell population growth was simulated for each experimental time interval and the relative growth rate constant was estimated from the slope of these simulated growth curves (Appendix A). Fig. 1C shows the algorithm for the population growth simulation. Note that TI_i was used instead of TP_i in the estimation of the growth rate constant.

Simulation of cell population growth curve: The simulation of cell population growth over time was performed using $TP_i(t)$ calculated from Eqs. (5.1) to (5.3), $F_i(t)$ obtained from cytometry and the same algorithm shown in Fig. 1C (Appendix B). In order to obtain a smooth profile instead of stepwise changes over the sampling time intervals, the TP_i for inbetween sampling times was estimated by interpolation assuming linear changes over time.

The present model assumes no cell death during cell cycle progression as mentioned above, hence, the model simulation represents a reduction in number of cells resulting from cell cycle arrest or disturbed cell cycle progression only. The model should underestimate the growth inhibition in the presence of cell death (number of cells killed) and the difference between the model-predicted and the observed growth curve of a treated cell population represents the growth inhibition resulting from cell death in the population.

RESULTS

Cytotoxicity and cell cycle arrest induced by UCN-01 In order to decide the drug concentration to use in our population growth inhibition study, the anti-proliferative effect of UCN-01 against SBC-3 cells was determined by MTT assay after 48- and 72-h drug exposures (data not shown). The greater cytotoxicity was seen for the longer

Table I. Concentration- and Time-dependent Changes in Cell Cycle Distribution and Transition Probability (TP_i) of SBC-3 Cells

UCN-01 (μM)	Time (h)	Percent of cells in			Transition probability[a] (h^{-1})		
		G_1	S	G_2/M	TP_{G1}	TP_S	$TP_{G2/M}$
0.2	0	31.5	44.8	23.6	0.271	0.140	0.215
	12	44.4	41.6	14.0	0.143	0.111	0.291
	24	54.0	30.2	15.8	0.112	0.159	0.262
	34	52.2	32.9	14.9	0.084	0.104	0.200
	48	52.1	33.3	14.6	0.104	0.127	0.252
2	0	30.4	42.9	26.7	0.289	0.153	0.194
	12	45.3	30.5	24.2	0.171	0.203	0.207
	24	60.7	20.0	19.2	0.092	0.239	0.209
	34	65.9	19.7	14.4	0.042	0.120	0.143
	48	67.7	17.9	14.5	0.057	0.186	0.201
0	34	32.7	41.8	25.5	0.216	0.127	0.166
0.1		44.6	38.0	17.4	0.138	0.122	0.227
0.2		52.2	32.9	14.9	0.100	0.124	0.238
0.5		56.4	26.0	17.6	0.091	0.161	0.202
1.0		60.2	21.7	18.1	0.075	0.176	0.179
2.0		65.9	19.7	14.4	0.058	0.166	0.199

The cell cycle distribution was determined by FACS analysis. Each concentration was evaluated in a separate experiment with its own control samples in tandem.
a) TP_{G1}, TP_S, and $TP_{G2/M}$ denote the transition probability from G_1 to S, S to G_2/M, G_2/M to G_1, respectively, which were calculated using Eqs. (5.1) through (5.3).

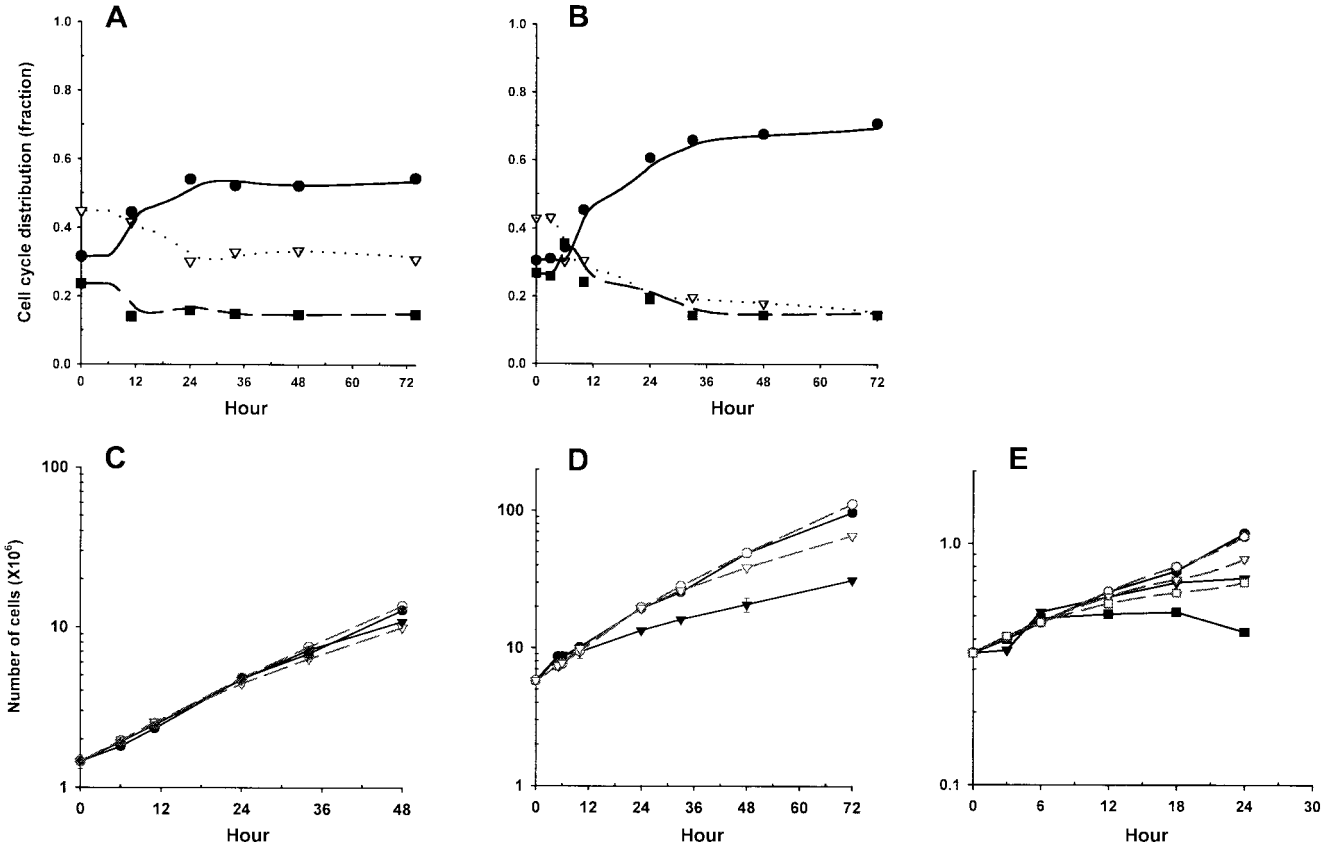

Fig. 2. Validation of the cytostatic TP_i model. (A) and (B) Comparison of the observed (symbols) and model-predicted (lines) cell cycle distributions among SBC-3 cells treated with UCN-01. (A) 0.2 μM, (B) 2 μM UCN-01 treatment. G_1 ●, S ▽, G_2/M ■. (C) and (D) Comparison of the observed (filled symbols with a solid line) and the model-predicted (open symbols with broken lines) cell population growth of SBC-3 cells following 0.2 μM (C) and 2 μM (D) UCN-01 exposure. Circles (●, ○) and triangles (▼, ▽) represent control and drug-treated cell population, respectively. (E) An example of an application of the cytostatic TP_i model. The observed data (filled symbols with a solid line) are compared to the model prediction (open symbols with broken lines) for Jurkat cells exposed to no drug (●, ○), 100 nM (▼, ▽) and 300 nM (■, □) UCN-01. The raw data were obtained from the reference.[19] Note that the *y*-axis is in log scale and that the SD of most data points is smaller than the symbol size.

exposure time as indicated by the lower IC_{50} (0.32 and 0.17 μM, respectively). The drug concentrations of 0.2 and 2 μM, which were close to $IC_{40,\,48\ h}$ and $IC_{90,\,72\ h}$, respectively, were selected.

The effect of UCN-01 on the cell cycle distribution was concentration- and exposure time-dependent (Table I). After 48 h exposure at 0.2 and 2 μM UCN-01, an accumulation in G_1 and a reduction in S phase were observed, and the changes were greater at the higher drug concentration, which was consistent with a previous study.[17] A decrease in the G_2/M fraction occurred to the same extent at both concentrations. When cells were exposed to 0.1 to 2 μM UCN-01 for 34 h, the decrease in the G_2/M phase fraction seemed to reach maximum at 0.1–0.2 μM, whereas other cell cycle arrest effects continued to increase up to the highest drug concentration tested (Table I). Significant changes in the cell cycle distribution were observed as early as 12 h post exposure, and a plateau was reached after 24 h for the 0.2 and 2 μM drug concentrations (symbols in Fig. 2, A and B).

Model validation Using the TP_i (described in 'Model development'), the cell cycle distribution (Fig. 2, A and B) and cell population growth (Fig. 2, C and D) of SBC-3 cells with or without drug exposure were simulated. The predicted data were compared with the observed data for validation of the present model.

Excellent agreement between the observed and the model-predicted cell cycle distribution was obtained for cells exposed to both 0.2 and 2 μM UCN-01 over 72 h (Fig. 2, A and B). Good agreement was also shown for population growth of cells with no drug treatment for 48 h (Fig. 2C) or for 72 h (Fig. 2D). These data indicate the

validity of the model to predict cell population growth using cell cycle distribution data in the absence of significant cell death.

When cells were treated with 0.2 μM UCN-01, no significant difference in population growth between untreated and treated cells was seen until 34 h and 22% decrease in cell number was observed after 48 h exposure (Fig. 2C). The reduced growth rate was well-predicted by the model simulation indicating that the growth inhibition (22%) may be fully accounted for by the cell cycle arrest effect, not by cell death.

For cells exposed to 2 μM UCN-01, significant reduction in population growth (i.e., decreased slope of treated compared to untreated cells) was observed at 24 h and the later time points (Fig. 2D). However, the model-predicted growth curve showed a significant reduction in cell number only at 48 and 72 h compared to the observed growth curve of untreated cells. These data indicate that the significant growth inhibition resulting from cell cycle arrest occurred after 48 h exposure, and the growth inhibition shown until 34 h may be accounted for by cell death, not by cell cycle arrest. Out of 73% growth inhibition shown at 72 h, 32% and 41% is accounted for by cell cycle arrest and cell death, respectively (as determined from the cell numbers at 72 h: 97.4×10^6 cells for observed control (●), 66×10^6 cells for model-prediction of treated population (▽), and 26.3×10^6 cells for observed treated population (▼) (Fig. 2D).

By comparing the model-predicted and the observed experimental data in SBC-3 cells (Fig. 2, A to D), the following information can be inferred. (i) UCN-01 induced cell cycle arrest as early as at 12 h after exposure (Fig. 2, A and B), but significant growth inhibition directly resulting from cell cycle arrest was not observed until 34 h post drug exposure regardless of drug concentration, which indicates that there is a delay between apparent changes in cell cycle distribution and subsequent population reduction, (ii) At 2 μM, the contribution of cell death to the overall growth inhibition decreased significantly after 48 h exposure, i.e., the slope of the observed growth curve gradually increased and approached that of the model-predicted curve: observed and model-predicted exponential growth rate constants for the 48–72 h interval were 0.0174 and 0.0224 h^{-1}, respectively, whereas at earlier time intervals, the observed growth rate constants were 2.3- to 2.5-fold lower than the predicted rates. (iii) The kinetics of growth inhibition resulting from cell death seemed different between 0.2 μM (no significant cell kill until 48 h) and 2 μM (significant cell kill after 12 h). This may be interpreted in terms of different cell death rates induced by the two different drug exposure conditions, as reported recently for 5-FU.[18]

Collectively, these data indicate that the present model is very useful in analyzing the relationship of cell cycle arrest or cell death with overall growth inhibition. It can thus provide detailed information about the cytotoxic mechanism of anti-proliferative agents.

Model application (Fig. 2E) In order to demonstrate the applicability and usefulness of the present model, a set of literature data was re-analyzed.[19] For TP_i calculation and growth simulation, the necessary data consisted of the cell cycle distribution changes over time (Table 2 in ref. 19) and the growth inhibition-time profile determined by viable cell number counting (Fig. 1 in ref. 19). The present TP_i model successfully predicted the growth of untreated Jurkat cells (Fig. 2E). In cells exposed to 100 nM UCN-01, the observed- and model-predicted data agreed until up to 18 h, but the model simulation overestimated the population growth at 24 h (Fig. 2E). This indicated that the growth inhibition resulted from the cell cycle arrest effect of UCN-01 during the first 18 h, and that significant cell death occurred only after 24 h of drug exposure at this drug concentration. At 300 nM, cell kill affected the population growth rate of Jurkat cells 12 h post exposure. At the end of 24 h drug exposure, 35% and 60% growth inhibition was observed in Jurkat cells exposed to 100 and 300 nM UCN-01, of which 22% and 37% could be attributed to drug-induced cell cycle arrest (Fig. 2E), respectively.

Comparison of growth inhibition by UCN-01 in SBC-3 vs. Jurkat cells UCN-01 induced significant cell cycle arrest 12 h post drug exposure in both SBC-3 and Jurkat cells (Fig. 2A and 2B, Table 2 in ref. 19). However, growth inhibition caused by cell cycle arrest was observed at an earlier time in Jurkat cells, i.e., 24 h in Jurkat cells vs. 48 h in SBC-3 cells. These data suggest that the mechanism underlying the cell cycle arrest in Jurkat cells is more effective in inducing growth inhibition.

Under drug exposure conditions causing significant growth inhibition (>50% inhibition), the contribution of cell cycle arrest to the overall growth inhibition was greater for Jurkat cells in comparison to SBC-3 cells. Sixty percent growth inhibition was seen for SBC-3 cells treated with 2 μM UCN-01 for 48 h vs. 7% for Jurkat cells treated with 300 nM UCN-01 for 24 h. Under these conditions, 22% and 37% of growth inhibition could be attributed to the cell cycle arrest effect of UCN-01 in SBC-3 and Jurkat cells, respectively (Fig. 2E). These data again indicate that Jurkat cells are not only more sensitive to the overall growth inhibitory effect of UCN-01, which may be due to primed apoptosis, but also that they are more prone to cell cycle arrest-mediated growth inhibition than the solid tumor cell line SBC-3.

Looking at the mechanism of cell cycle arrest in more detail (Table II), the data show that UCN-01 induced a significant decrease (74%) in TP_{G1} with a concomitant increase in TP_S (29%) and $TP_{G2/M}$ (13%) in SBC-3 cells, resulting in G_1 accumulation and S and G_2/M reduction. In contrast, a significant decrease (71%) in TP_S with an

Table II. Comparison of UCN-01-induced Cell Cycle Arrest between SBC-3 Cells and Jurkat Cells[a)]

Cell line	UCN-01	Exposure time (h)	Transition probability[d)] (% change compared to control)		
			TP_{G1}	TP_S	$TP_{G2/M}$
SBC-3	0 μM	48	0.218	0.144	0.178
	0.2 μM[b)]		0.104 (−52.3)	0.127 (−11.8)	0.252 (+41.6)
	2 μM[b)]		0.057 (−73.9)	0.186 (+29.2)	0.201 (+12.9)
Jurkat[a)]	0 μM	24	0.214	0.192	0.333
	100 nM[c)]		0.169 (−21.0)	0.112 (−41.7)	0.450 (+35.1)
	300 nM[c)]		0.210 (−1.9)	0.055 (−71.4)	0.465 (+39.6)

The cell cycle distribution was determined by FACS analysis.
a) Data for Jurkat cells were taken from the ref. 19).
b) The values 0.2 and 2 μM represent $IC_{20,\ 48\ h}$ and $IC_{70,\ 48\ h}$, respectively, at a seeding density of 4000 cells/well as determined by MTT assay in the present study.
c) The values 100 and 300 nM represent $IC_{70,\ 24\ h}$ and $IC_{90,\ 24h}$, respectively.[19)]
d) TP_{G1}, TP_S, and $TP_{G2/M}$ denote the transition probability from G_1 to S, S to G_2/M, G_2/M to G_1, respectively, which were calculated using Eqs. (5.1) through (5.3).

increase (40%) in $TP_{G2/M}$ was induced in Jurkat cells, resulting in G_2/M phase abrogation. Although an apparently similar change in the cell cycle distribution is observed, the underlying mechanism may be different, as shown by the TP_i analysis. Different mechanisms of drug-induced cell cycle arrest may in turn explain the different rates and degrees of the contribution of cell cycle arrest to the overall growth inhibition.

DISCUSSION

For many anticancer agents with classical mechanisms of action such as DNA alkylation and microtubule binding, apoptotic cell death has been considered a secondary event resulting from drug-induced macromolecular damage and subsequent cell cycle arrest. However, recent studies have suggested that the signal transduction pathways leading to cell cycle arrest or cell death, especially apoptosis, may be independent. For example, it has been shown that paclitaxel-induced cell death occurs via a signaling pathway independent of microtubules and G_2/M arrest.[20, 21)] It has been difficult to study each pathway independently of the other, because the two phenomena often occur simultaneously and no method had been available to assess their respective contributions to the overall growth inhibition under certain drug treatment conditions. As mentioned in the introduction section, cell death including apoptosis is an elimination process for which there is no cumulative index for convenient use. In contrast, cell cycle arrest is relatively easier to study using flow cytometric DNA histogram analysis. The present study was undertaken to develop a novel method that can extract quantitative information from cell cycle distribution data (fraction of cells in each phase) and also exploit it for the assessment of growth inhibition directly resulting from cytostatic effects of anticancer agents. Here, we report the development of a novel computational model that can be used to predict growth inhibition resulting from cell cycle arrest, so that one can easily evaluate the contribution of the counterpart, cell death, to the overall growth inhibition under given cytotoxic conditions.

Transition probability theory, proposed by Smith and Martin[12)] and widely used in many modeling studies, is the basis for the present model as described under "Materials and Methods": the main model parameter, TP_i was derived from Smith and Martin's transition probability theory and successfully used to analyze in detail the mechanism of cell cycle arrest in the present study. Another key element of the present model is the consideration of the age structure of a simple exponential population by Steel.[16)] In the simulation of a growth curve, the transitions of cells between cell cycle phases were modeled as a probabilistic procedure (i.e., based on TP_i, Appendix B). However, to estimate the growth rate constant, the relative transition probabilities, TI_i, were used (Appendix A). In this numerical simulation, the distribution of cells within each phase also determines the transition rate of cells and thus eventually the growth rate of the population. In other words, the number of cells transiting per one transition event depends on the distribution of cells at each age (or step) within the phase. Without the consideration of the age structure, the model simulation would produce false growth patterns, e.g. unrealistic fluctuations in the cell cycle distribution during cell population growth.

The UCN-01-induced growth inhibition measured in terms of viable cell count showed some difference from the MTT assay data. The 0.2 μM treatment ($IC_{40,\ 48\ h}$ by MTT) showed only 22% growth inhibition by viable cell

count, instead of 40% following a 48-h exposure. The 2 μM treatment ($IC_{90, 72\ h}$, MTT assay) showed 73% inhibition instead of 90% after 72 h of exposure (MTT data not shown, see Fig. 2 for viable cell counts). In order to explain this discrepancy, we examined the effect of various seeding densities on MTT assay results. By increasing the seeding density from 2000 cells/well to 4000 cells/well, the $IC_{50, 48\ h}$ was increased from 0.32 to 0.9 μM. By increasing the density to 4000 cells/well good agreement of percent growth inhibition was achieved between the MTT vs. direct cell count data, i.e., 20% (vs. 22%) and 75% (vs. 73%) growth inhibition was determined for the 48-h ecxposure at 0.2 μM, and the 72-h exposure at 2 μM, respectively (MTT data not shown, see Fig. 2 for viable cell counts). These data suggest that the UCN-01-induced cytotoxicity is significantly influenced by the seeding density, which may be due to the decreased intracellular drug concentration secondary to the depletion of the drug in the medium, as has been shown for paclitaxel.[22)]

In summary, a novel computational model (we would like to call it the "cytostatic TP_i model") was developed and validated for detailed analysis of cell cycle arrest and prediction of the population growth of cancer cells under cytostatic conditions. The growth inhibition predicted by the TP_i model represents the decrease in population growth resulting directly from a cell cycle perturbation effect, i.e., cell cycle block. The present model uses the discrete time Markov model, and hence, it avoids mathematical complexity. It provides a simple new method to assess the relative contributions of cell cycle arrest and cell kill to the overall anti-proliferative effect of anticancer agents.

We propose that this novel method can be applied to study in detail the mechanisms of cell cycle arrest and its contribution to overall growth inhibition induced by new anticancer agents and/or new combination therapies. A template simulation program is included in the appendix to aid researchers who are interested in using this model in their studies.

ACKNOWLEDGMENTS

This work was supported in part by Grants-in-Aid for Cancer Research from the 2nd Term Comprehensive 10-Year Strategy for Cancer Control, the Japanese Ministry of Health and Welfare, and the Japanese Ministry of Education, Science, Sports and Culture. H.-J. Kuh is a recipient of an international scientific cooperation fellowship from the Foundation for Promotion of Cancer Research, Japan. J. Usuda is a recipient of a research resident fellowship from the Foundation for Promotion of Cancer Research, Japan.

(Received May 24, 2000/Revised August 16, 2000/Accepted September 6, 2000)

REFERENCES

1) Akinaga, S., Nomura, K., Gomi, K. and Okabe, M. Diverse effects of indolocarbazole compounds on the cell cycle progression of ras-transformed rat fibroblast cells. *J. Antibiot. (Tokyo)*, **46**, 1767–1771 (1993).
2) Akinaga, S., Nomura, K., Gomi, K. and Okabe, M. Effect of UCN-01, a selective inhibitor of protein kinase C, on the cell-cycle distribution of human epidermoid carcinoma, A431 cells. *Cancer Chemother. Pharmacol.*, **33**, 273–280 (1994).
3) Kawakami, K., Futami, H., Takahara, J. and Yamaguchi, K. UCN-01, 7-hydroxylstaurosporine, inhibits kinase activity of cyclin-dependent kinases and reduces the phosphorylation of the retinoblastoma susceptibility gene product in A549 human lung cancer cell line. *Biochem. Biophys. Res. Commun.*, **219**, 778–783 (1996).
4) Sausville, E. A., Lush, R. D., Headlee, D., Smith, A. C., Figg, W. D., Arbuck, S. G., Senderowicz, A. M., Fuse, E., Tanii, H., Kuwabara, T. and Kobayashi, S. Clinical pharmacology of UCN-01: initial observation and comparison to preclinical models. *Cancer Chemother. Pharmacol.*, **42**, S50–S54 (1998).
5) Seynaeve, C. M., Stetler-Stevenson, M., Sebers, S., Kaur, G., Sausville, E. A. and Worland, P. J. Cell cycle arrest and growth inhibition by the protein kinase antagonist UCN-01 in human breast carcinoma cells. *Cancer Res.*, **53**, 2081–2086 (1993).
6) Bunch, R. T. and Eastman, A. 7-Hydroxystaurosporine (UCN-01) causes redistribution of proliferating cell nuclear antigen and abrogates cisplatin-induced S-phase arrest in Chinese hamster ovary cells. *Cell Growth Differ.*, **8**, 779–788 (1997).
7) Wang, Q., Fan, S., Eastman, A., Worland, P. J., Sausville, E. A. and O'Connor, P. M. UCN-01: a potent abrogator of G2 checkpoint function in cancer cells with disrupted p53. *J. Natl. Cancer Inst.*, **88**, 956–965 (1996).
8) Shao, R. G., Cao, C. X., Shimizu, T., O'Connor, P. M., Kohn, K. W. and Pommier, Y. Abrogation of an S-phase checkpoint and potentiation of camptothecin cytotoxicity by 7-hydroxystaurosporine (UCN-01) in human cancer cell lines, possibly influenced by p53 function. *Cancer Res.*, **57**, 4029–4035 (1997).
9) Eastman, A., DiPetrillo, K. J. and Brown, M. K. Abrogation of irinotecan-mediated S and G2 arrest by 7-hydroxystaurosporine (UCN-01) and the impact of p53 status. *Proc. Am. Assoc. Cancer Res.*, **40**, 305 (1999).
10) Shi, Z. and Plunkett, W. Induction of apoptosis without cell cycle progression by UCN-01 abrogates gemcitabine induced S phase arrest in human myeloid ML-1 cells. *Proc. Am. Assoc. Cancer Res.*, **40**, 305 (1999).
11) Morikage, T., Ohmori, T., Nishio, K., Fujiwara, Y., Takeda,

Y. and Saijo, N. Modulation of cisplatin sensitivity and accumulation by amphotericin B in cisplatin-resistant human lung cancer cell lines. *Cancer Res.*, **53**, 3302–3307 (1993).
12) Smith, J. A. and Martin, L. Do cells cycle?, *Proc. Natl. Acad. Sci. USA*, **70**, 1263–1267 (1973).
13) Robinson, J. H., Smith, J. A., Totty, N. F. and Riddle, P. N. Transition probability and the hormonal and density-dependent regulation of cell proliferation. *Nature*, **262**, 298–300 (1976).
14) Shields, R. Further evidence for a random transition in the cell cycle. *Nature*, **273**, 755–758 (1978).
15) Shields, R., Brooks, R. F., Riddle, P. N., Capellaro, D. F. and Delia, D. Cell size, cell cycle and transition probability in mouse fibroblasts. *Cell*, **15**, 469–474 (1978).
16) Steel, G. G. Growth kinetics of tumors. "Cell Population Kinetics in Relation to the Growth and Treatment of Cancer," pp. 59–61 (1977). Clarendon Press, Oxford.
17) Akiyama, T., Yoshida, T., Tsujita, T., Shimizu, M., Mizukami, T., Okabe, M. and Akinaga, S. G1 phase accumulation induced by UCN-01 is associated with dephosphorylation of Rb and CDK2 proteins as well as induction of CDK inhibitor p21/Cip1/WAF1/Sdi1 in p53-mutated human epidermoid carcinoma A431 cells. *Cancer Res.*, **57**, 1495–1501 (1977).
18) Brown, J. M. and Wouters, B. G. Apoptosis, p53, and tumor cell sensitivity to anticancer agents. *Cancer Res.*, **59**, 1391–1399 (1999).
19) Wang, Q., Worland, P. J., Clark, J. L., Carlson, B. A. and Sausville, E. A. Apoptosis in 7-hydroxystaurosporine-treated T lymphoblasts correlates with activation of cyclin-dependent kinases 1 and 2. *Cell Growth Differ.*, **6**, 927–936 (1995).
20) Johnson, K. R., Wang, L., Miller, M. C., 3rd, Willingham, M. C. and Fan, W. 5-Fluorouracil interferes with paclitaxel cytotoxicity against human solid tumor cells. *Clin. Cancer Res.*, **3**, 1739–1745 (1997).
21) Fan, W. Possible mechanisms of paclitaxel-induced apoptosis. *Biochem. Pharmacol.*, **57**, 1215–1221 (1999).
22) Kuh, H.-J., Jang, S. H., Tran, A. Q., Wientjes, M. G. and Au, J. L.-S. Computational model of intracellular pharmacokinetics of paclitaxel. *J. Pharmacol. Exp. Ther.*, **293**, 761–770 (2000).

APPENDIX

A. An example of a Fortran program for estimation of cell growth rate K using TI_i

```
      Implicit real*8 (a-h,o-z)
      REAL N1, N2, N3, ND1, ND2, ND3, NT
      INTEGER TIME, CK, C10, TD, MFNmax
      OPEN (UNIT=10, STATUS='OLD',FILE='In.DAT')
      OPEN (UNIT=20, STATUS='OLD',FILE='Out.DAT')
      READ (10,*) P10, P20, P30, C10, TD, MFNmax
      WRITE (20,95) P10, P20, P30, C10,TD, MFNmax
 95   Format('P10=', F5.3, 3X, 'P20=', F5.3, 3X, 'P30=',
     + F5.3, 3X, 'C10=', I5, 3X, 'TD=', I5, 3X, 'MFNmax=',I5)
C Define TI(i)
      TI_1=P20*P30/(P10*P20+P20*P30+P30*P10)
      TI_2=P30*P10/(P10*P20+P20*P30+P30*P10)
      TI_3=P10*P20/(P10*P20+P20*P30+P30*P10)
      P1=P10
      P2=P20
      P3=P30
      PP1=P1
      PP2=P1+P2
      T30=(1./LOG(2.))*LOG(1.+P3)
      T20=(1./LOG(2.))*LOG(1.+P2+P3)-T30
      T10=1.-T20-T30
      T1=T10
      T2=T20
      T3=T30
      PS1=T10
      PS2=T10+T20
      C1=C10
      NT=0.5*C1*(1./(1.-2.**(-1./TD)))
      N1=NT*P1
      N2=NT*P2
      N3=NT*P3
      Nmax=MFNmax*NT
      Time=0
      CK=0
C Iteration Loop for entire set
      C Print*, 'Check=',Check, TP_1,TP_2,TP_3
      40 Call RANDOM_number(Check)
      IF (Check. LE. PP1) then
      GOTO 50
      Else if (Check. LE. PP2) then
      GOTO 60
      Else
      GOTO 70
      END IF
C Iteration for each set
 50   CALL RANDOM_number(TP_1)
      IF (TI_1. GE. TP_1) Then
      ND1=C1*(2.**(-1./TD*(T1*TD-1.)))
      N1=N1-ND1
      N2=N2+ND1
      NT=N1+N2+N3
      Else
      End If
      GOTO 400
 60   CALL RANDOM_number(TP_2)
      IF (TI_2. GE. TP_2) Then
      ND2=C1*(2.**(-1./TD*((T1+T2)*TD-1.)))
      N2=N2-ND2
      N3=N3+ND2
      NT=N1+N2+N3
```

```
      Else
      End If
      GOTO 400
 70   CALL RANDOM_number(TP_3)
           IF (TI_3. GE. TP_3) Then
           ND3=C1*(2.**(−1./TD*(TD−1.)))
           N3=N3-ND3
           N1=N1+2.*ND3
           NT=N1+N2+N3
      C1=2.*ND3
      Else
           End If
           GOTO 400
400   P1=N1/NT
      P2=N2/NT
      P3=N3/NT
      PP1=P1
      PP2=P1+P2
      T3=(1./LOG(2.))*LOG(1.+P3)
      T2=(1./LOG(2.))*LOG(1.+P2+P3)–T3
      T1=1.-T2-T3
      PS1=T1
      PS2=T1+T2
      IF (Time. EQ. (1000*CK)) THEN
      Write (20,90) Time, N1,N2,N3,NT,P1,P2,P3
 90   Format (I7, 4F10.0, 3F10.3)
      CK=CK+1
      ELSE
      ENDIF
      IF (NT. LT. Nmax) Then
           TIME=TIME+1
           GOTO 40
           Else
           End If
      write  (*,*)'Time=',TIME,  'N1=',N1,'N2=',N2,'N3=',N3,
      'NT=',NT
      STOP
      END
```

B. An example of a Fortran program for cell growth simulation using TP_i

```
      Implicit real*8 (a-h,o-z)
      REAL N1, N2, N3, NT, NN1, NN2, NN3
      INTEGER TIME, MFNmax
      OPEN (UNIT=10, STATUS='OLD', FILE='In.DAT')
      OPEN (UNIT=20, STATUS='OLD', FILE='Out.DAT')
      READ (10,*) TP10, TP20, TP30, NT0, P10, P20, P30,
      MFNmax
      WRITE (20,95) TP10, TP20, TP30, NT0, P10, P20, P30,
      MFNmax
 95   Format('TP10=', F5.3, 1X, 'TP20=', F5.3, 1X, 'TP30=',
      +F5.3, 1X, 'NT0=', I7, 1X, 'P10=', F5.3, 1X, 'P20=',
      +F5.3, 1X, 'P30=', F5.3, 1X, 'MFNmax=',I3 )
 C    TP_i can be written as a time function
      TP1=TP10
      TP2=TP20
      TP3=TP30
      P1=P10
      P2=P20
      P3=P30
      N1=NT0*P1
      N2=NT0*P2
      N3=NT0*P3
      NT=NT0
      Nmax=MFNmax*NT0
      Time=0
 30   Write (20,90) Time,N1,N2,N3,NT,P1,P2,P3
 90   Format(I5, 4F10.0, 3F7.3)
      Time=TIME+1
 C    Add intrapolation eqn for TP_i
      IF (TIME. LE. 3) Then
      TP12=0.262+(0.256-0.262)/3*(TIME)
      TP22=0.139+(0.137-0.139)/3*(TIME)
      TP32=0.176+(0.181-0.176)/3*(TIME)
      TP1=TP12
      TP2=TP22
      TP3=TP32
      ELSE IF (TIME. LE. 6) Then
      TP13=0.256+(0.238-0.256)/3*(TIME-3)
      TP23=0.137+(0.221-0.137)/3*(TIME-3)
      TP33=0.181+(0.139-0.181)/3*(TIME-3)
      TP1=TP13
      TP2=TP23
      TP3=TP33
      ELSE IF (TIME. LE. 10) Then
      TP14=0.238+(0.155-0.238)/4*(TIME-6)
      TP24=0.221+(0.185-0.221)/4*(TIME-6)
      TP34=0.139+(0.188-0.139)/4*(TIME-6)
      TP1=TP14
      TP2=TP24
      TP3=TP34
ELSE IF (TIME. LE. 24) Then
      TP15=0.155+(0.079-0.155)/14*(TIME-10)
      TP25=0.185+(0.205-0.185)/14*(TIME-10)
      TP35=0.188+(0.179-0.188)/14*(TIME-10)
      TP1=TP15
      TP2=TP25
      TP3=TP35
      ELSE IF (TIME. LE. 33) Then
      TP16=0.079+(0.063-0.079)/9*(TIME-24)
      TP26=0.205+(0.178-0.205)/9*(TIME-24)
      TP36=0.179+(0.213-0.179)/9*(TIME-24)
      TP1=TP16
      TP2=TP26
      TP3=TP36
      ELSE IF (TIME. LE. 48) Then
      TP17=0.063+(0.058-0.063)/15*(TIME-33)
      TP27=0.178+(0.189-0.178)/15*(TIME-33)
      TP37=0.213+(0.205-0.213)/15*(TIME-33)
      TP1=TP17
      TP2=TP27
      TP3=TP37
      ELSE IF (TIME. LE. 72) Then
      TP18=0.058+(0.050-0.058)/24*(TIME-48)
      TP28=0.189+(0.215-0.189)/24*(TIME-48)
      TP38=0.205+(0.188-0.205)/24*(TIME-48)
      TP1=TP18
      TP2=TP28
      TP3=TP38
```

```
ELSE
TP1=0.050
TP2=0.215
TP3=0.188
ENDIF
      NN1=N1-N1*TP1+2*N3*TP3
      NN2=N2-N2*TP2+N1*TP1
NN3=N3-N3*TP3+N2*TP2
      N1=NN1
      N2=NN2
N3=NN3
      NT=N1+N2+N3
P1=N1/NT
P2=N2/NT
P3=N3/NT
IF (NT. LT. Nmax) Then
      GOTO 30
      ELSE
      ENDIF
write  (*,*)'Time=',TIME,  'N1=',N1,'N2=',N2,'N3=',N3,
'NT=',NT
STOP
END
```